ELSEVIER

Biochimica et Biophysica Acta 1188 (1994) 318–324

BBA Biochimica et Biophysica Acta

An ENDOR study of structural changes in the environment of the dark stable tyrosine radical, $Y_D^{\cdot}$, of Photosystem 2 induced by inhibition of the oxygen evolving complex

Stephen E.J. Rigby [a], Dugald J. Maclachlan [a], Jonathan H.A. Nugent [a,*], Patrick J. O'Malley [b]

[a] *Department of Biology, Darwin Building, University College London, Gower Street, London WC1E 6BT, UK*
[b] *Department of Chemistry, UMIST, P.O. Box 88, Manchester M60 1QD, UK*

Received 30 August 1994

Abstract

The oxygen evolving complex (OEC) of Photosystem II (PS II) may be inhibited without inducing the loss of the manganese cofactor. Methods include depletion of the calcium cofactor by high salt concentration and the addition of ammonium ions at alkaline pH or acetate ions at acidic pH. ENDOR spectra of the dark stable tyrosine radical $Y_D^{\cdot}$ in PS II have been obtained for samples treated in these ways. These show that the orientation of the tyrosine aromatic ring relative to the attached β methylene protons is different in each case. The effects are specific to the inhibitory treatment employed and have been quantitated. Y_D is constrained by its protein environment and as such these orientation effects show that the protein environment around this tyrosine is affected by such inhibitory treatments. Since the distance between the OEC and Y_D has previously been estimated at 3–4 nm (Evelo, R.G., Styring, S., Rutherford, A.W. and Hoff, A.J. (1989) Biochim. Biophys. Acta 973, 428–442), the ENDOR data suggest that long-range protein-mediated communication occurs between them. The orientation of Y_D is also shown to be sensitive to the removal of the light harvesting complex, LHC II.

Keywords: Photosystem II; ENDOR; Tyrosine radical; Oxygen evolving complex

1. Introduction

Photosystem II (PS II) is a multiprotein complex of the thylakoid membrane [1]. It functions as a water : plastoquinone oxidoreductase and contains several redox cofactors, both organic and inorganic. Tyrosine radicals in PS II are generated by the action of the oxidising species $P680^+$, the photogenerated cation of the primary donor. Two such tyrosine radicals have been identified by using site-directed mutagenesis in cyanobacteria [2–5]. One of these, Y_Z, constitutes the link between P680 and the oxygen evolving complex (OEC) by which it is re-reduced [6]. The other, Y_D, while able to oxidise the OEC slowly in the dark, is stable in the oxidised state for hours [6,7]. Y_D has been identified as Tyr 161 of the D2 protein. The D1 and D2 proteins of PS II are thought to form a 1 : 1 complex with C2 symmetry analogous to the L/M complex of the bacterial reaction centre from which models of D1/D2 can be made [8,9]. The distance between Y_D and the OEC has been estimated at 3–4 nm from the relaxation enhancement effect of the OEC on the electron spin relaxation times of $Y_D^{\cdot}$ [10]. The OEC contains a minimum of four manganese ions and is thought to be the site of water oxidation [11]. During the catalytic cycle the OEC is oxidised in four successive one electron steps. The oxidation states are referred to as S_x states where x indicates the number of one electron steps and varies from 0 (fully reduced) to 4 (fully oxidised) [12]. Calcium [13] and chloride [14,15]

Abbreviations: ENDOR, electron nuclear double resonance; EPR, electron paramagnetic resonance; Hepes, 4-(2-hydroxyethyl)-1-piperazineethanesulfonic acid; HTG, *n*-heptyl thioglucoside; LHC II, the light harvesting chlorophyll complex associated with PS II; MES, 2-[*N*-morpholino]ethanesulfonic acid; OEC, the manganese-containing oxygen evolving complex of PS II; P680, the primary donor chlorophyll(s) of PS II; PS II, Photosystem II; Tris, tris-(hydoxymethyl)aminomethane Y_D, the dark stable tyrosine radical (D2 161) of PS II; $Y_Z^{\cdot}$, the tyrosine radical (D1 161) that transfers electrons between the OEC and P680.

* Corresponding author. Fax: +44 71 3807096.

SSDI 0005-2728(94)00140-5

ions have been identified as cofactors in the water oxidation process. They are intimately associated with the OEC and their depletion perturbs the catalytic cycle.

Calcium-depleted PS II forms a dark stable S_2 state and from this state only one further electron may be removed from the donor side, so that oxygen evolution is inhibited. The dark stable S_2 state gives rise to a modified multiline EPR spectrum [16–19] (^{55}Mn induced splitting of 5.5 mT compared to 7.5–9 mT for uninhibited PS II [20]). Oxidation of S_2 generates a new EPR spectrum at the expense of the multiline. This new spectrum, which consists of a 16 mT wide derivative centred around $g = 2$, has been variously ascribed to the interaction between a histidine radical and the OEC (S_2 state) [16,21] or the interaction between $Y_Z^{\cdot}$ and the OEC (S_2 state) [19]. A proportion of the molecules may attain the 'true' S_3 state of the OEC [22]. Thus the source of the third electron removed from the OEC is still debatable. While it is not the purpose of this communication to resolve such debates, this description of calcium-depleted PS II shows that calcium removal perturbs the structure of the OEC.

Ammonia is thought to bind to at least two sites in the OEC. One of these competes with the chloride ion [23,24]. Under the conditions of high chloride and low sucrose concentration, ammonia binds not at a chloride site but to a second site where it directly co-ordinates the manganese cluster [25]. Ammonia-treated PS II shows greatly reduced rates of $Y_Z^{\cdot}$ reduction, implying disruption of electron transfer between Y_Z and the OEC. The S_2 state of ammonia-treated PS II again has a modified multiline EPR spectrum (^{55}Mn splitting of 7 mT) [24]. Furthermore, oxidation of this state removes the multiline spectrum and reveals a new spectrum consisting of a broad line (roughly) 10 mT wide with no resolved structure, centred around $g = 2$ [19,26]. Again the source of this spectrum is not known definitively, but the implications for structural changes at the OEC are evident.

Acetate also inhibits oxygen evolution by binding at the OEC, probably at sites normally occupied by chloride ions. No dark stable multiline is formed in the presence of this inhibitor, but oxidation to the level of the S_3 state produces a new spectrum centred at $g = 2$ with a linewidth of approx. 22 mT [27]. The stoichiometry and binding site for acetate are as yet unknown. Consistent with the behaviour of the inhibitors described above, these observations suggest that acetate also affects the OEC structure.

Oxygen evolution is completely inhibited by removal of the manganese ions of the OEC. This can be achieved by washing with high concentrations of Tris at high pH, typically 1 M at pH 8.8 [28]. PS II treated in this way shows no S_2 or S_3 state EPR spectra and no oxygen evolution. The extrinsic polypeptides associated with the OEC (the 33, 23 and 17 kDa proteins) are also removed by such Tris treatment.

Since tyrosine radicals are paramagnetic, they can be studied using EPR (electron paramagnetic resonance) and ENDOR (electron nuclear double resonance) spectroscopies. ENDOR enables hyperfine coupling constants to be measured far more accurately than EPR, and also allows for the detection of small hyperfine couplings to which the powder EPR spectrum is largely insensitive. Tyrosine radicals provided the first EPR spectra to be associated with PS II [29]. The spectra are anisotropically broadened, with small g anisotropy and partially resolved hyperfine structure. The EPR spectrum of $Y_D^{\cdot}$, once formed in the dark, may be frozen for studies at cryogenic temperatures. Such low temperatures are necessary for the implementation of the ENDOR technique.

Previously, we have assigned many of the resonances in the ENDOR spectrum of $Y_D^{\cdot}$ and determined the hyperfine coupling constants for all four ring protons and both β methylene protons [30]. We have shown [30] that the orientation of the aromatic ring of $Y_D^{\cdot}$ is different in PS II from different species. These changes arise from interspecies variation in the protein structure around Y_D. Such sensitivity suggests that orientation of $Y_D^{\cdot}$ could be used as a local structural probe of the effects of site-directed mutagenesis or chemical modification on PS II. Here we report studies using ENDOR spectroscopy in which the spectrum of $Y_D^{\cdot}$ is shown to be sensitive to treatments which specifically inhibit the OEC, which is 3–4 nm distant [10], and to treatment with n-heptyl thioglucoside (HTG) which removes the light harvesting chlorophyll a/b complex (LHC II), producing an oxygen-evolving core preparation [31].

2. Materials and methods

PS II membranes, BBYs [32], were prepared from market spinach by the method of Ford and Evans [33]. Calcium depletion was as given in Hallahan et al. [19] with reconstitution of the extrinsic polypeptides. Ammonia-treated samples were also prepared as in Ref. [19] in the presence of high chloride concentrations. To increase the number of centres to which ammonia was bound, these samples were annealed as in Ref. [19]. Acetate treatment was as given in Ref. [27]. BBYs were depleted of manganese and the donor side extrinsic polypeptides by Tris washing (1 M, pH 8.8) as in Ref. [28]. HTG particles were produced using the method of Ref. [31].

Samples were 15–20 mg Chl/ml in 0.3 M sucrose, 10 mM NaCl, 20 mM MES or Hepes at pH 5.5, 6.5 or 7.5. Acetate-treated samples produce maximal trapped

S3 state at pH 5.5 and ammonia-treated samples at pH 7.5. The ENDOR spectra of such samples were better defined at these optimal pH values. Other samples (native, calcium-depleted, Tris-washed and HTG-treated) exhibited pH-independent ENDOR spectra over this pH range. Typical sample volumes were 150 μl in 3 mm i.d. quartz tubes. ENDOR spectra were obtained at X-band using a Bruker ESP 300 EPR spectrometer in conjunction with a Bruker EN 003 ENDOR interface, Wavetec 3000–446 radio frequency synthesizer, EN 370 power amplifer, and EN 801 ENDOR cavity (estimated Q of 800). The Wavetec synthesizer also provided for frequency modulation of the radio frequency output. Spectra were obtained at 10 K (helium flow), temperature control being effected using an Oxford instruments continuous flow ESR 900 cryostat with an ITC 4 temperature controller. The impedance of the radio frequency circuit was 50 Ω. ENDOR spectra were corrected for baseline nonlinearity by the subtraction of off-resonance scans which were filtered for noise (standard Bruker software) to avoid reducing the spectrum signal to noise ratio. Acquisition conditions for specific spectra are given in the figure captions. The reproducibility of hfc determination was ± 0.05 MHz.

3. Results

ENDOR resonance assignments were made according to Ref. [30]. ENDOR enhancements for Tris-washed PS II were considerably smaller than those of manganese sufficient preparations due to the affect of the paramagnetic OEC on the electron and nuclear spin relaxation times of $Y_D^{\cdot}$. ENDOR spectra of $Y_D^{\cdot}$ covering the range 20–33 MHz, in oxygen-evolving native BBY PS II particles and four inhibited states of PS II are shown in Fig. 1. These spectra were recorded with 158 kHz r.f. modulation depth. The resonances 3 and 4 arise from the A_z features of the inequivalent ring protons at positions 3 and 5 (A_z 3,5 = 19.1 and 21.5 MHz) (see Fig. 2 for the tyrosine numbering scheme). These resonances are unaffected by the inhibitory treatments. Resonances 2 and 1 are the $A_\perp$ and $A_\parallel$ features respectively of the larger of two β proton hyperfine couplings. These resonances occur at different frequencies in each of the five species studied, Table 1. The smaller coupling constants of the tyrosine radical are difficult to resolve at high r.f. modulation depth. Therefore high resolution (28 kHz r.f. modulation depth) ENDOR spectra were obtained for each of the species in Fig. 1. Parts of these spectra covering the range 15.5–20 MHz are shown in Fig. 3. The β proton $A_\parallel$ resonances are visible at approx. 19 MHz, feature 5. The β proton $A_\perp$ resonances are superimposed on the A_x components of the inequivalent 2 and 6 position ring protons at approx. 16.5 MHz (A_x 2,6 = 4.4 and 4.8 MHz), feature 8. While the two contributions to the spectrum in this region are difficult to separate, changes in this region which correlate with changes in the β proton $A_\parallel$ are evident and can be revealed using difference spectra [30]. The 2,6 proton A_y features are labelled 7 (A_y 2,6 = 7.15 and 7.4 MHz) and the visible part of the broad 3,5 proton, A_y turning point (A_y 3,5 = 8.0 MHz) is labelled 6. As with the 3,5 proton couplings, the 2,6 proton couplings are the same in all the species of Fig. 3. The spectra of the inhibited species exhibit no heterogeneity, suggesting that conversion to the inhibited form is quantitative. Note that although the symmetry related pairs of ring protons, 2,6 and 3,5, have inequivalent hyperfine couplings, it is not possible to assign particular coupling constants to a particular proton within each pair. The

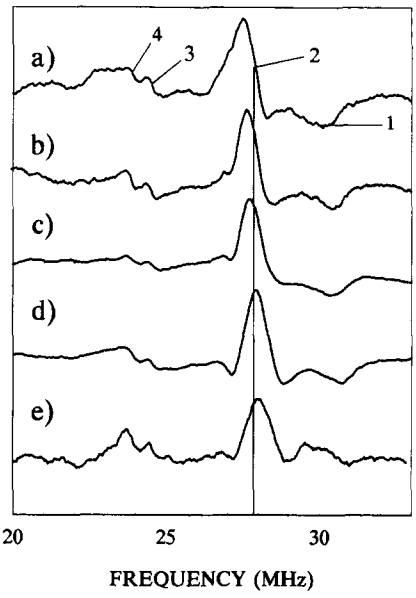

Fig. 1. ENDOR spectra of the $Y_D^{\cdot}$ covering the range 20–33 MHz in (a) native, (b) acetate-inhibited, (c) ammonia-inhibited, (d) calcium-depleted and (e) Tris-washed PS II. Spectra recorded with 10 mW microwave power, 100 W r.f. power and 158 kHz r.f. FM modulation depth, at 10 K. Numbers refer to features discussed in the text. Vertical reference line set at the native BBY β proton $A_\perp$.

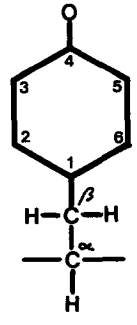

Fig. 2. Numbering scheme for the carbon atoms of the tyrosine neutral radical.

Table 1
β-Methylene proton hyperfine coupling constants (MHz) as a function of PS II treatment

	β_1		β_2	
	$A_\perp$	$A_\parallel$	$A_\perp$	$A_\parallel$
Native	27.2	31.5	4.6	9.8
Acetate-inhibited	27.2	31.7	4.5	9.8
Ammonia-inhibited	27.6	32.1	4.3	9.6
Calcium-depleted	28.1	32.6	4.0	9.4
Tris-washed	28.3	33.1	3.9	9.2
HTG-treated	27.7	32.3	4.3	9.5

3,5 protons A_x feature is hidden under the axial system of the large β proton coupling. Using orientation selection ENDOR taken at the low field (g_x) edge of the EPR spectrum, we have previously shown [30] that for $Y_D^{\cdot}$ in spinach BBY preparations A_x 3,5 has two components (in keeping with the behaviour of 3,5 A_z) with hyperfine couplings of -25.6 MHz and -27.5 MHz. The calcium-depleted preparation is the most perturbed of those studied here that retains a full complement of manganese ions. These ions provide for large ENDOR enhancements through increased $Y_D^{\cdot}$ electron and nuclear spin relaxation. Therefore orientation selection experiments have been performed on calcium-depleted PS II to determine the 3,5 A_x position and to confirm the β proton assignments in these inhibited PS II preparations. Since calcium-depleted PS II is the most perturbed manganese sufficient preparation, it seems reasonable to extrapolate these results to less perturbed states. The spectra, Fig. 4,

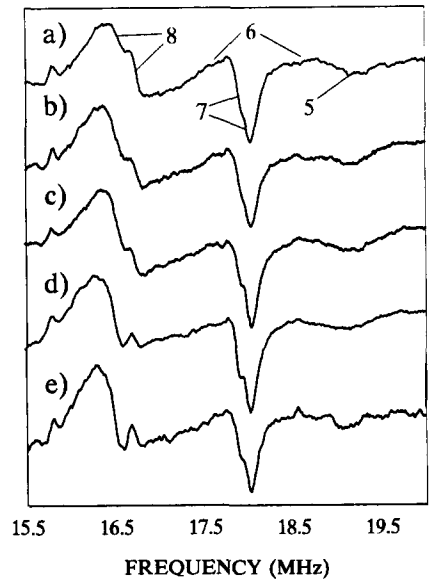

Fig. 3. ENDOR spectra of the $Y_D^{\cdot}$ covering the range 15.5–20 MHz in (a) native, (b) acetate-inhibited, (c) ammonia-inhibited, (d) calcium-depleted and (e) Tris-washed PS II. Spectra recorded with 6.3 mW microwave power, 63 W r.f. power and 28 kHz r.f. FM modulation depth, at 10 K. Numbers refer to features discussed in the text.

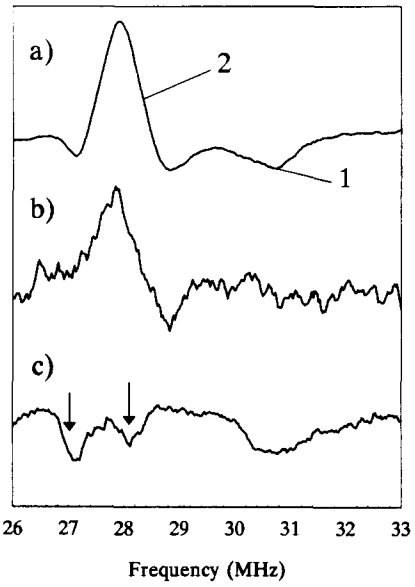

Fig. 4. ENDOR spectra of $Y_D^{\cdot}$ in calcium-depleted PS II with the field setting at (a) the EPR spectrum crossing point, (b) at the high field edge of the EPR spectrum (g_z), (c) at the low field edge of the EPR spectrum (g_x). Parameters as Fig. 1 but with a r.f. FM modulation depth of 199 kHz for (b) and (c). Numbers refer to features discussed in the text. The A_x components of the inequivalent 3,5 proton hyperfine tensors are marked with arrows.

confirm the assignments of the β proton couplings (features 1 and 2) and show that the 3,5 A_x (arrowed in the Fig.) is not altered in the inhibited states. The principle axes of the β proton hyperfine tensor have been shown, by simulation of the EPR spectra of $Y_D^{\cdot}$ deuterated at the 3 and 5 positions, to be oriented such that $A_\parallel$ is approximately colinear with g_x while $A_\perp$ is in the g tensor y-z plane [30,34].

HTG treatment removes both LHC II and one calcium ion [31]. The loss of this calcium ion is not associated with a loss of oxygen evolution activity [31]. The ENDOR spectrum of $Y_D^{\cdot}$ in HTG treated PS II is shown in Fig. 5a and d. The 3,5 proton couplings are identical to those of BBYs (feature 3 and 4), but the large β proton coupling (features 1 and 2) is unique, Table 1. Addition of calcium ions to this preparation had no effect on the ENDOR spectrum of $Y_D^{\cdot}$, Fig. 5b. Calcium-depleted HTG preparations, Fig. 5c, however, have a $Y_D^{\cdot}$ ENDOR spectrum identical to that of calcium depleted BBYs, Fig. 1d.

The region of the ENDOR spectrum of $Y_D^{\cdot}$ around the free proton frequency υ_p (a region often referred to as the matrix region) arises from hyperfine coupling between the unpaired electron and protons on the protein. The tyrosine α proton will also contribute resonances in this region [35]. Matrix region ENDOR spectra of $Y_D^{\cdot}$ at 10 K in native BBY and inhibited forms are shown in Fig. 6. While none of the resonances in this region can be definitively assigned to particular protons, this region reflects the state of the

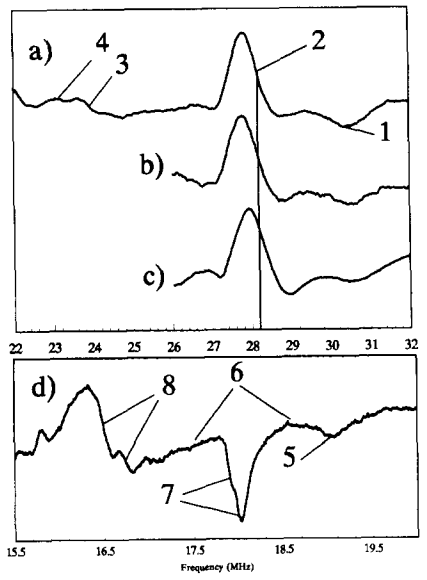

Fig. 5. ENDOR spectra of $Y_D^{\cdot}$ in HTG-treated PS II with (a) no additions, (b) with the addition of 10 mM calcium ions ($CaCl_2$), (c) after calcium depletion of (a). Spectrum (d) is a high resolution ENDOR spectrum of HTG-treated PS II. The spectra (a–c) were recorded using the same parameters as Fig. 1 and spectrum (d) used the same parameters as Fig. 2. Numbers refer to features discussed in the text. Vertical reference line is set at the β proton $A_\perp$ observed in HTG-treated samples with no additions, (a).

protein environment around the tyrosine radical. The inhibited states exhibit various degrees of resonance broadening relative to the native BBY spectrum. This is illustrated by the decreased resolution of the inhibited state spectra and changes in the relative intensities

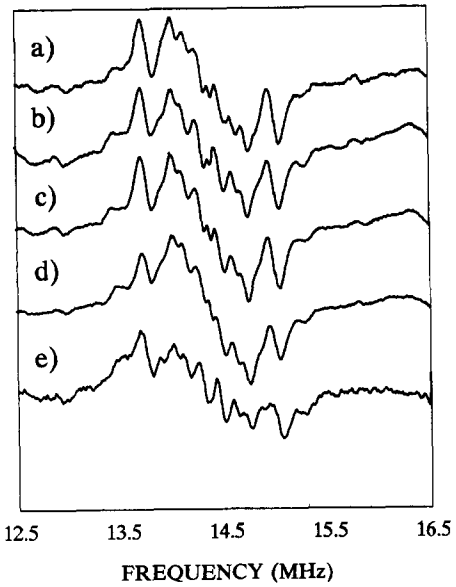

Fig. 6. ENDOR spectra of $Y_D^{\cdot}$ covering the matrix region, 12.5–16.5 MHz in (a) native, (b) acetate-inhibited, (c) ammonia inhibited, (d) calcium-depleted and (e) Tris-washed PS II. Spectra were recorded with 6.3 mW microwave power, 63 W r.f. power and 35 kHz r.f. FM modulation depth at 10 K.

of the resonances. Such effects are particularly evident in the spectra of calcium-depleted and Tris-washed PS II, Figs. 6d and e.

While changes in the oxidation state (S-state) of the OEC affected the relative intensities of the ENDOR resonances, in keeping with the known affects of S-state on the electron spin relaxation times of $Y_D^{\cdot}$ [10] (and hence the nuclear spin relaxation times also), no S-state dependent changes in hyperfine coupling constants were observed for any species.

4. Discussion

The ENDOR spectra of $Y_D^{\cdot}$ in each of the states studied here show different β-methylene proton hyperfine couplings, while the ring proton couplings remain the same in all the spectra. These effects are specific to the treatment employed and there is no evidence for heterogeneity in any of the spectra. The ENDOR spectrum of $Y_D^{\cdot}$ in HTG-treated samples suggests that the environment of Y_D is also sensitive to events occurring at the interface between the PS II core and LHC II (Fig. 5). That the effect of HTG treatment on $Y_D^{\cdot}$ ENDOR is through a calcium-depletion effect on HTG-treated samples is excluded by the failure of added calcium to restore the BBY $Y_D^{\cdot}$ spectrum (Fig. 5b).

The β proton coupling constants depend on both the electron spin density at carbon 1 (ρC1) and the orientation of the aromatic ring relative to the β protons [36], i.e. the β proton conformational angle θ, Fig. 7. The contributions to the coupling from ρC1 and θ can be separated using the McConnell relation [37]:

$$A_{iso} = B\rho\cos^2\theta$$

where A_{iso} is the isotropic hyperfine coupling constant, B is a constant equal to 162 MHz, ρ is the paramagnetic electron spin density at C1, and θ is the angle between the normal to the ring plane and the plane formed by C1, Cβ and the β proton i.e the conformational angle of the β proton. Note that the value of θ for the proton with the large coupling constant is denoted θ_1, while for the proton with the smaller coupling constant is θ_2, and therefore θ_2 is equivalent to $120 - \theta_1$, assuming tetragonal symmetry at Cβ [30, 34,38].

Solving this equation for $Y_D^{\cdot}$ in the six PS II species studied here leads to the data of Table 2. This shows that the perturbations in the spectra induced on inhibition arise from small rotations of the tyrosine ring relative to the β protons, ρC1 remaining constant. The θ values are different for each inhibition treatment studied. Therefore each treatment has a characteristic effect on $Y_D^{\cdot}$. EPR spectra of $Y_D^{\cdot}$ at room temperature show that even at such temperatures the ring of tyro-

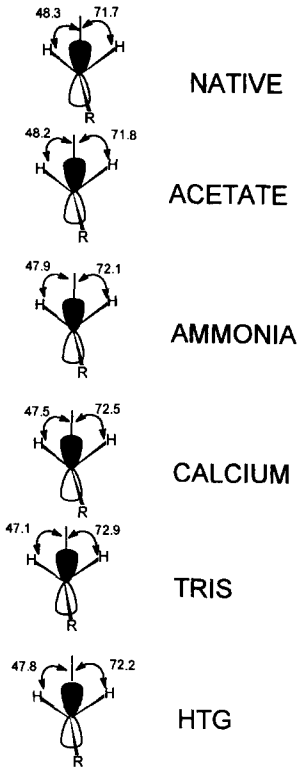

Fig. 7. Schematic representation of the β-methylene proton dihedral angles, θ, of $Y_D^{\cdot}$ for the treatments studied. The view is looking down along the β- carbon to ring carbon 1 bond in Fig. 1.

sine Y_D is constrained by the protein [39]. Therefore even the small changes in θ reported here must arise as a consequence of rearrangements in the protein surrounding Y_D. This conclusion is supported by the behaviour of the matrix region of the ENDOR spectrum. Resonances in the matrix region of the spectrum arise principally from protein protons (the resonances arising from the protons on the tyrosine α carbon also occur in this region [35], but they are difficult to assign without specific deuteration). A well defined matrix region suggests a very well defined protein environment. Such a spectrum is exhibited by the native BBY sample, Fig. 6a. Where the protein environment is more mobile, the coupling constants vary on the timescale of the experiment leading to line broadening as in Fig. 6d and e. Thus the dynamics of the protein environment are altered in the inhibited species suggesting subtle rearrangements. The dynamics of the tyrosine ring itself are apparently not altered, the linewidths and resolution being the same for all those features arising from ring or β protons regardless of treatment. This is particularly evident in the 2,6 proton couplings where the observation of non-degenerate couplings for these two protons is expected to depend critically on the rotational dynamics of the tyrosine ring.

Table 2
Methylene angles, θ, and C1 spin densities as a function of PS II treatment

	θ_1	θ_2	ρC1
Native	48.3°	71.7°	0.4
Acetate-inhibited	48.2°	71.8°	0.4
Ammonia-inhibited	47.9°	72.1°	0.4
Calcium-depleted	47.5°	72.5°	0.4
Tris-washed	47.1°	72.9°	0.4
HTG-treated	47.8°	72.2°	0.4

The S3 state EPR spectrum has been assigned to an OEC-radical interaction showing weak electron spin exchange (and also presumably electron-electron dipolar) coupling [16,21]. The exchange and dipolar interactions are dependent on the relative geometry (distance, bond lengths and angles) of the two paramagnets. This suggests that the different S3 spectra produced by the various inhibitors could arise from the interaction of the same manganese-radical combination, but with these centres having a different relative geometry in each case. The conformation changes detected in the ENDOR of $Y_D^{\cdot}$ provide a mechanism for such structural variation between inhibited species and therefore a possible explanation for S3 spectrum variation.

Predicted structures of the D1/D2 heterdimer suggest the OEC is bound to the lumenal side C terminus of D1 [8–9]. Taken with the distance between the OEC and Y_D determined from electron spin relaxation measurements (3–4 nm) [10], this implies that the effects observed here are transmitted by a network of interacting amino acid residues including those at the D1/D2 interface. Thus two regions of PS II separated by nm distances and on different polypeptides are mechanically (and/or if electrostatic interactions are involved, electromechanically) connected. While the effects reported here have little impact on the function or behaviour of Y_D, these data do provide evidence for information transmission through the protein matrix of PS II. This has important consequences for the study of regulation of PS II by effectors (e.g. covalent phosphorylation) acting at a site distant from the redox active centres and for studies using site-specific mutagenesis.

Acknowledgement

We acknowledge funding from the U.K. Science and Engineering Research Council.

References

[1] Anderson, B. and Styring, S. (1991) Curr. Top. Bioenerg. 16, 1–81.
[2] Debus, R.J., Barry, B.A., Babcock, G.T. and McIntosh, L. (1988) Proc. Natl. Acad. Sci. USA 85, 427–430.

[3] Debus, R.J., Barry, B.A., Sithole, I., Babcock, G.T., and McIntosh, L. (1988) Biochemistry 27, 9071–9074.
[4] Vermass, W.F.J., Rutherford, A.W. and Hansson, O. (1988) Proc. Natl. Acad. Sci. USA 85, 8477–8481.
[5] Metz, J.G., Nixon, P.J., Rogner, M., Brudvig, G.W. and Diner, B.A. (1989) Biochemistry 28, 6960–6969.
[6] Babcock, G.T., Barry, B.A., Debus, F.J., Hoganson, C.W., Atamian, M., McIntosh, L., Sithole, I. and Yocum, C.F. (1989) Biochemistry 28, 9557–9565.
[7] Styring, S. and Rutherford, A.W. (1987) Biochemistry 26, 2401–2405.
[8] Svensson, B., Vass, I., Cedergren, E. and Styring, S. (1990) EMBO J. 7, 2051–2059.
[9] Ruffle, S.V., Donnelly, D., Blundell, T.L. and Nugent, J.H.A. (1992) Photosynth. Res. 34, 287–300.
[10] Evelo, R.G., Styring, S. Rutherford, A.W. and Hoff, A.J. (1989) Biochim. Biophys. Acta 973, 428–422.
[11] Debus, R.J. (1992) Biochim. Biophys. Acta 1102, 269–352.
[12] Kok, B., Forbush, B. and McGloin, M.P. (1970) Photchem. Photobiol. 11, 457–475.
[13] Yocum, C.F. (1991) Biochim. Biophys. Acta 1059, 1–15.
[14] Critchley, C. (1985) Biochim. Biophys. Acta 811, 33–46.
[15] Coleman, W.J. (1990) Photosynth. Res. 23, 1–27.
[16] Boussac, A., Zimmermann, J.L. and Rutherford, A.W. (1989) Biochemistry 28, 8984–8989.
[17] Ono, T. and Inoue, Y. (1989) Physiol. Plant. 76, A141.
[18] Sivaraja, M., Tso, J. and Dismukes, G.C. (1989) Biochemistry 28, 9459–9464.
[19] Hallahan, B.J., Nugent, J.H.A., Warden, J.T. and Evans, M.C.W. (1992) Biochemistry 31, 4562–4573.
[20] Dismukes, G.C. and Siderer, Y. (1981) Proc. Natl. Acad. Sci. USA 78, 274–278.
[21] Boussac, A., Zimmermann, J.L., Rutherford, A.W. and Lavergne, J. (1990) Nature 347, 303–306.
[22] Maclachlan, D.J., Nugent, J.H.A. and Evans, M.C.W. (1994) Biochim. Biophys. Acta 1185, 103–111.
[23] Sandusky, P.O. and Yocum, C.F. (1983) FEBS Lett 162, 339–343.
[24] Beck, W.F. and Brudvig, G.W. (1987) Biochemistry 26, 8285–8295.
[25] Britt, R.D., Zimmermann, J.L., Sauer, K. and Klein, M.P., (1989) J. Am. Chem. Soc. 111, 3522–3532.
[26] Andréasson, L.E. and Lindberg, K. (1992) Biochim. Biophys. Acta 1100, 177–183.
[27] Maclachlan, D.J. and Nugent, J.H.A. (1993) Biochemistry 32, 9772–9780.
[28] Kuwabara, T. and Murata, N. (1983) Plant Cell Physiol. 24, 741–747.
[29] Commoner, B., Heise, J.J. and Townsend, J. (1956) Proc. Natl. Acad. Sci. USA 42, 710–718.
[30] Rigby, S.E.J., Nugent, J.H.A. and O'Malley, P.J. (1994) Biochemistry 33, 1734–1742.
[31] Enami, I., Kamino, K., Shen, J.-R., Satoh, K. and Katoh, S. (1989) Biochim. Biophys. Acta 977, 33–39.
[32] Berthold, D.A., Babcock, G.T. and Yocum, C.F. (1981) FEBS Lett. 134, 231–234.
[33] Ford, R.C. and Evans, M.C.W. (1983) FEBS Lett. 160, 159–163.
[34] Hoganson, C.W. and Babcock, G.T. (1992) Biochemistry 31, 11874–11880.
[35] Sealy, R.C., Harman, L., West, P.R. and Mason, R.P. (1985) J. Am. Chem. Soc. 107, 3401–3406.
[36] Fessenden, R.W. and Schuler, R.H. (1963) J. Chem. Phys. 39, 3147.
[37] McConnell, H.M. (1956) J. Chem. Phys. 24, 764.
[38] Bender, C.J., Sahlin, M., Babcock, G.T., Barry, B.A., Chandrashekar, T.K., Salowe, S.P., Stubbe, J., Lindström, B., Petersson, L., Ehrenberg, A. and Sjöberg, B.-M. (1989) J. Am. Chem. Soc. 111, 8076–8083.
[39] Barry, B.A. and Babcock, G.T. (1987) Proc. Natl. Acad. Sci. USA 84, 7099–7103.